Thomson scattering at general fusion

W. C. Young[a] and D. Parfeniuk
General Fusion, Burnaby, British Columbia V3N 4T5, Canada

(Presented 8 June 2016; received 6 June 2016; accepted 30 June 2016;
published online 11 August 2016)

This paper provides an overview of the Thomson scattering diagnostic in use at General Fusion, including recent upgrades and upcoming plans. The plasma experiment under examination produces temperatures in the 50-500 eV range with density on the order of 10^{20} m^{-3}. A four spatial point collection optics scheme has been implemented, with plans to expand to six spatial points. Recent changes to the optics of the laser beamline have reduced stray light. The system employs a frequency doubled Nd:YAG laser (532 nm), a grating spectrometer, and a photomultiplier array based detector. *Published by AIP Publishing.* [http://dx.doi.org/10.1063/1.4959915]

I. INTRODUCTION

General Fusion is working towards a magnetized target fusion reactor that compresses a compact toroid within an acoustically collapsed vortex of liquid metal.[1,2] Demonstrating the ability to compress a compact toroid to fusion conditions is a top priority of developing this scheme. In current compression tests, a collapsing metal vessel serves as a proxy for the liquid metal vortex. However, this configuration provides limited diagnostic access to the plasma. The compression tests are supplemented by heavily diagnosed, but uncompressed laboratory tests. The extra diagnostics and faster shot repetition of these lab tests provide a testbed for development of experimental parameters and characterizing conditions to be used in compression tests. Thomson scattering is a critical diagnostic of these lab tests, as the temperature of the plasma prior to adiabatic compression, along with compression ratio, determines the final temperature reached.

Described below are the components of the Thomson scattering diagnostic installed on General Fusion's newest machine: SPECTOR. The geometry of this machine is intended to test spherically symmetric compression and is illustrated in Figure 1.

II. LASER OPTICS

A. Laser

The diagnostic uses a commercial, almost off-the-shelf Nd:YAG laser as a light source: a Spectra-Physics Quanta-Ray Pro-370. This is a factory modification of the stock Pro-350 model that produces nearly twice the pulse energy of ~2 J at 532 nm. During recent operation, the pulse energy varies from 1.5 to 1.85 J due to day-to-day variation in the alignment of the second-harmonic generator. The second harmonic is used due to the spectral sensitivities of the current and previous scattered light detectors.

The laser operates at 10 Hz, allowing for only a single temperature measurement within a plasma shot of typical millisecond duration. The plasma experiment produces a flashlamp trigger asynchronous to the 10 Hz cycle. The *q*-switch is then triggered relative to the breakdown time of the plasma, which includes some jitter relative to flashlamp timing. This triggering method allows for better timing relative to reproducible plasma phenomena, but results in shot-to-shot variation in pulse energy. Under typical conditions, the resulting jitter between q-switch and flashlamp pulse has an RMS value of 13 μs. Larger variations up to several tens of microseconds are possible when exploring conditions that impacted breakdown time and were more common on older machines. A photodiode behind a turning mirror compensates for the pulse energy variation in density calculations. Between the timing jitter, asynchronous triggering, and the lasers own variation, the pulse-to-pulse energy variation has a typical RMS of about 10%.

B. Beamline and stray light

The laser beamline should focus down to a fixed scattering volume, while reducing stray laser light that can very easily overwhelm the small scattered signal. To improve long time scale alignment stability, motorized mirror mounts (Newport AG-M100N adapted to 2 in. optics) were incorporated. By monitoring the beam location at two points with inexpensive cameras, slow drifts in the beam position can be corrected between plasma shots without interrupting the plasma experiment cycling.

To improve stray light reduction, a new set of optics were installed based on stray light reduction on the Pegasus experiment.[3] Instead of employing numerous annular baffles to reduce propagation of light scattered off of the entrance window and other surfaces, two conical baffles are used, each, for the entrance and exit, as shown in Figure 2. This simplifies construction and potentially the alignment of the

Note: Contributed paper, published as part of the Proceedings of the 21st Topical Conference on High-Temperature Plasma Diagnostics, Madison, Wisconsin, USA, June 2016.

[a]Author to whom correspondence should be addressed. Electronic mail: william.young@generalfusion.com.

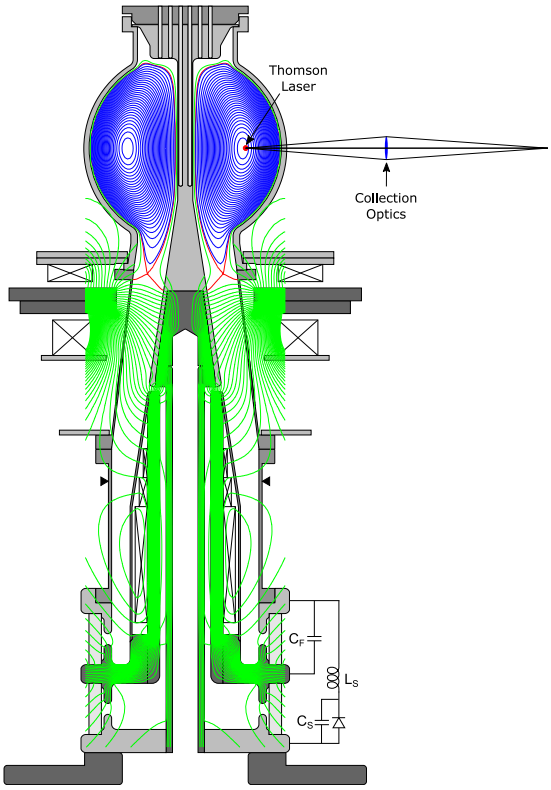

FIG. 1. A vertical cross-section of the SPECTOR machine is shown, with predicted equilibrium magnetic field lines. The Thomson scattering laser beam position is shown to be in the compact toroid midplane near the magnetic axis, with horizontal collection optics (some viewports are tilted above or below the midplane, see Figure 2).

system, especially considering the second baffle has loose alignment tolerances (3-4 mm radially, vs. 1 mm radially for the first baffle).

This baffle system ensures any scattered light requires multiple bounces off of optically blackened surfaces before reaching the inner, reflective vacuum vessel surface that could scatter light into collection optics. By designing the entrance and exit tubes to trap light coming from the plasma volume, the baffles do not need to block all scattered light and instead only need to restrict scattered light to a cone that will enter the opposing tube. The combination of two baffles' inner radii is chosen to be as large as possible while blocking any direct path from the entrance window to the inner vacuum vessel. Additionally the second baffle will block any ray from the edge of the first baffle to the inner vacuum vessel. In other words, there is no line of sight from the entrance window and first baffle's edge to anywhere on the inner surface of the vacuum vessel.

The interior of the entrance and exit tubes is optically blackened to help trap light. Vacuum and plasma compatibility limits blackening choices. The current implementation uses Aquadag, a colloidal graphite suspended in water and ammonia that can be applied with spray painting equipment. After baking, a vacuum compatible and mechanically stable graphite coating remains. However, misalignment of the laser easily strips off the coating, often on surfaces critical to reduction of stray light, e.g., the edge of the baffle. Any future revision of this design may be improved by using machined graphite instead of graphite coated stainless steel to prevent laser damage from reducing light absorption.

The long beamline vacuum tube also allows for a long focal length lens, f = 1.5 m, for minimizing the beam size over multiple viewpoints. The entrance and exit windows of the beamline are Brewster angle mounts holding optical grade windows, as opposed to previously used generic vacuum viewports normal to the beam. After the exit, a beam dump is constructed of two sets of neutral density filters at the Brewster angle followed by a razor blade light dump.[4] The net result of the new baffle system, entrance window, and dump is a rough factor 3-5 reduction in stray light with a much simpler construction. However, the previous installation was on a different machine with different internal geometry making direct comparison difficult. As seen in Figure 3, the stray light is low compared to the signal in a typical shot.

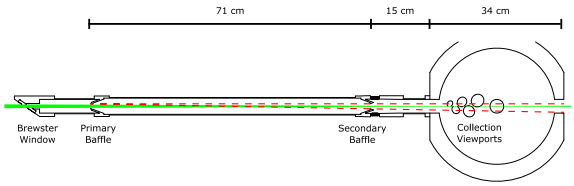

FIG. 2. The above diagram shows a scale vertical cross-section vacuum entrance optics, stray light baffles, and collection optics viewports. The vacuum components have been simplified for clarity. The focusing laser beam (solid green) comes from a focusing lens in air off the left side then passes through a Brewster window into vacuum. The combination of the two baffles blocks all direct rays from the window and edge of the first baffle from reaching the interior of the vacuum vessel, ensuring stray light must make at least one reflection off graphite coated surface. Unblocked scattered light from the edge of the first baffle is shown as confined to the exit port (dashed red cone). The arrangement of the six collection viewports is shown to the right. All viewports are conical bores with the same apex angle, but appear as different sized circles due to the spherical vacuum vessel shape. The vacuum vessel has an inner diameter of 38 cm, but appears smaller in the cross-section as the Thomson scattering laser has a 12 cm offset from the center (see Figure 1).

III. COLLECTION OPTICS

As the vacuum vessel is a critical component of the electrical and magnetic circuits, a single large collection window was not considered feasible. With an ultimate goal of six spatial points, six conical bored holes were made in the

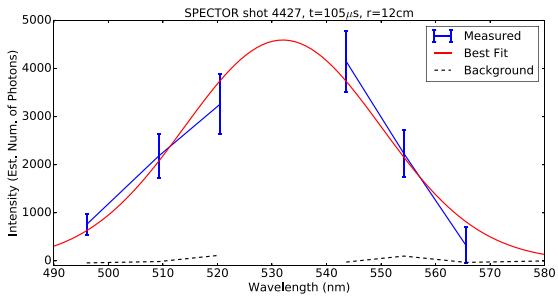

FIG. 3. An example shot and temperature fit ($T_e = 290 \pm 50$ eV) are displayed above for a single spatial point. The stray light is measured from a shot without plasma and scaled by laser pulse intensity. The vertical axis is scaled to the number of photons measured in each detector spectral bin, as estimated from photomultiplier specifications.

vacuum vessel, covered with a single large quartz window, including a shutter system for use during lithium coating. This mechanical setup constrains the collection optics, with minimum distances of 16 cm to the first optical component.

The current collection optics reuses components from a previous system, with only a 2 in., f = 150 mm lens per spatial point concentrating light onto an imaging fiber. Only four of the six potential positions are used with this setup, as the close proximity of the viewports does not provide enough room for independent lenses without sacrificing numerical aperture (NA). In the near future, this collection optics setup will be replaced with a single large condensing lens and additional correction lens to allow all six views to be used.

An imaging fiber that splits into 6 inputs is used for transporting the collected light to detectors. Each of the six channels has a 2×1.5 mm rectangular input area, with a limited NA of 0.14 chosen to match the spectrometer used in the detector setup.

IV. DETECTORS

The output of the imaging fiber is directed into the imaging slit of an imaging, $f/4.1$ spectrometer (Horiba iHR 320). The spectrometer has three gratings, 300, 600, and 1200 lines/mm, with the 600 lines/mm typically useful to temperatures up to ~500 eV. A physical block is used on the output of the spectrometer to remove the laser wavelength from the spectrum output. This does produce some leakage of stray light that is calibrated for and subtracted from measured spectra.

An array of photomultiplier tubes is used at the spectrometer output for converting the light signal into electrical signals. For multi-spatial point setups, an 8×8 array is used (Hamamatsu H7546A-20), giving seven spectral points for each spatial view (one lost behind laser line block). As plasma light is strong enough to deplete the dynode voltages if the photomultipliers were on for the entire shot, the first dynode is gated to a window about the Thomson laser firing time. The photomultiplier outputs are AC coupled into a bank of oscilloscopes to digitize the signals (at 1 GS/s with 200 MHz bandwidth).

V. CONCLUSIONS AND FUTURE PLANS

The latest implementation of Thomson scattering diagnostic has demonstrated the ability to measure electron temperature on General Fusion's newest machine. The hardware and data analysis structure are capable of measuring electron density, having done so on previous machines, however, Rayleigh scattering calibrations have not been done yet on the new machine.

Without the Rayleigh scattering calibration, an estimate can still be made of the collection efficiency. The number of photons at the detector has been estimated using the typical values for the photomultiplier tube's gain and photocathode current. This estimate is used to provide the vertical scale in Figure 3. This can be compared to the number of photons expected from the plasma (e.g., a 290 eV plasma, n_e of about 2×10^{20} m^{-3} plasma for the shot in Figure 3) and taking into account the limited collection area of a 50.8 mm lens located about 30 cm from the laser. The resulting photon efficiency from collection lens to photomultiplier tube is approximately 5%-15%, with large losses likely due to the grating efficiency and collection misalignment (only coarse alignment was done at this time, with finer alignment, along with Rayleigh scattering calibration, postponed to a later date). Nonetheless, due to the high plasma density, even with the low throughput, significant signal is obtained using a convenient and relatively inexpensive off-the-shelf spectrometer-based setup.

In the near term, further upgrades are planned with emphasis on increasing signal to noise ratio and resolving temperature gradients. A new collection optics setup will allow for six spatial points and more efficient light collection. The beamline is configured for an upgrade to multipass Thomson scattering with a few additional components.[5]

ACKNOWLEDGMENTS

On behalf of the General Fusion team we acknowledge the years of work by our former colleague Dr. Dean Parfeniuk in the development of Thomson scattering diagnostics at General Fusion. Dean's intellect, dedication, and passion for fusion were an inspiration to us all.

We would also like to thank Adrian Wong and Curtis Gutjahr for their work on General Fusion's Thomson scattering hardware.

[1]D. Richardson, A. Froese, V. Suponitsky, M. Reynolds, and D. Plant, in Proceedings of the 34th Annual Conference of the Canadian Nuclear Society, 2013, available at http://www.generalfusion.com/blog/wp-content/uploads/2014/07/General-Fusion-CNS-2013.pdf.
[2]M. Laberge, J. Fusion Energy **27**, 1 (2008).
[3]D. J. Schlossbergy, M. W. Bongard, R. J. Fonck, N. L. Schoenbeck, and G. R. Winz, J. Instrum. **8**, 11 (2013).
[4]D. J. Den Hartog and M. Cekic, Meas. Sci. Technol. **5**, 1115 (1994).
[5]R. Yasuhara *et al.*, Rev. Sci. Instrum. **83**, 10E326 (2012).